NUMERICAL AND THEORETICAL INVESTIGATIONS ON DETONATION-INERT CONFINEMENT INTERACTIONS

Tariq D. Aslam and John B. Bdzil
Los Alamos National Laboratory
Los Alamos, NM 87545
phone: 1-505-667-1367, fax: 1-505-667-6372
aslam@lanl.gov
jbb@lanl.gov

It is well known that the confinement of a high explosive (HE) cylinder by inert materials can change the detonation speed in the HE. The hydrodynamic basis of this effect can be understood by examining the pressure/streamline-deflection matching condition at the HE/inert interface. Although a full hydrodynamic simulation of the complete flow is needed for a detailed description of this interaction, a relatively simple shock polar analysis provides a good leading-order prediction of the confinement effect. Here, studies of various detonation-inert confinement interactions are examined from both a theoretical and computational point-of-view.

INTRODUCION AND THEORY

It is well known that the confinement of a high explosive (HE) cylinder by inert materials can change the detonation speed in the HE. The hydrodynamic basis of this effect can be understood by examining the pressure/streamline-deflection matching condition at the HE/inert interface. Although a full hydrodynamic simulation of the complete flow is needed for a detailed description of this interaction, a relatively simple shock polar analysis provides a good leading-order prediction of the confinement effect. The shock polar analysis considers matching the flow states (pressure and streamline deflection) that are found immediately behind the lead shocks (see Fig. 1). This is usually done in a frame of reference that moves with the detonation shock-inert interface intersection. To carry out the analysis, the equation of state of the unreacted HE and inert are required as well as an assumed value for the detonation phase speed.

The equations used for this analysis stem from the shock conditions of the Euler equations. The shock polar relates the post-shock pressure and the commensurate streamline deflection angle induced by an oblique shock wave. For an ideal gas (in the strong shock limit), given an initial density, ρ_o, and a phase speed, D_o, and ratio of specific heats, γ, one can determine the post shock pressure, p, and streamline deflection angle, ϕ, as a function of the shock deflection angle, ω:

$$p = \frac{2\rho_o D_o^2 \cos^2\omega}{\gamma+1}$$

$$\phi = \arctan\left(\frac{\sin\omega\cos\omega}{\gamma+1-2\cos^2\omega}\right)$$

The shock polar is given simply as a curve in p-ϕ space parameterized by the shock deflection angle, ω, which ranges from 0°

deflection to 90° deflection. At ω =0°, we recover the normal post shock pressure, and no streamline deflection. As ω is increased, the post shock pressure decreases, and the streamline deflection increases. There exists a maximum streamline deflection angle for a given shock deflection angle, at which point further increases in the shock deflection angle result in decreasing streamline deflection. For an ideal gas, this point corresponds to the point where the post shock state is exactly sonic in the steady reference frame. At ω =90°, the pressure and streamline deflection are zero, corresponding to an acoustic wave of zero strength. See Fig. 1 for two examples.

In general, there are several types of interactions that give a "match" of the pressure and streamline-deflection across the HE/inert interface. A match would simply be a point in p-ϕ space where the HE polar and inert polar cross. The two classical types of interactions are for strong and weak confinement.

For the typical strong confinement case, a lead shock in the HE is transmitted into the inert, with no reflected wave traveling back into the HE. See Fig. 1. There is a subsonic region behind the detonation shock, and a supersonic region behind the inert shock. The shock polar diagram for this case is shown in Fig. 2.

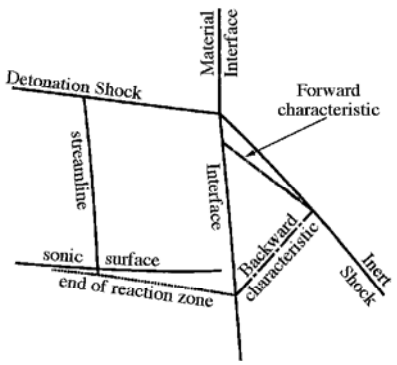

FIGURE 1. TYPICAL STRONG CONFINEMENT CONFIGURATION.

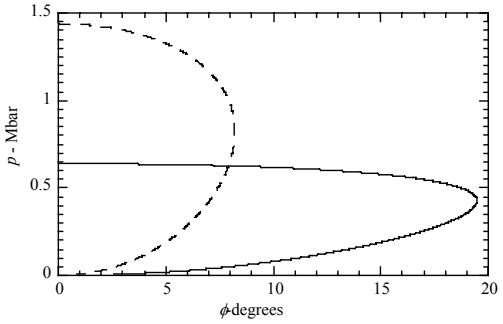

FIGURE 2. TYPICAL STRONG CONFINEMENT SHOCK POLAR. SOLID LINE IS HE POLAR (γ=3,ρo=2gm/cc,D_o=0.8cm/us), DASHED LINE IS INERT POLAR (γ=7,ρo=9gm/cc,D_o=0.8cm/us).

For the typical weak confinement case, the match between the higher pressure lead shock in the HE and the lower pressure transmitted shock in the inert requires an intervening Prandtl-Meyer expansion fan in the HE. See Figure 3. The associated shock polar, in Figure 4, shows that there

is no intersection of only shocks, and the only match occurs with a fan in the HE.

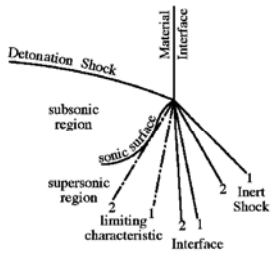

FIGURE 3. TYPICAL WEAK CONFINEMENT CONFIGURATION.

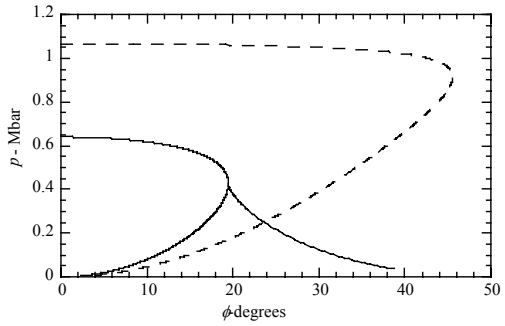

FIGURE 4. TYPICAL WEAK CONFINEMENT SHOCK POLAR. SOLID LINE IS HE POLAR (γ=3,ρo=2gm/cc,D_o=0.8cm/us), DASHED LINE IS INERT POLAR (γ=1.4,ρo=2gm/cc,D_o=0.8cm/us).

Numerical simulations, that resolve the pressure and streamline deflection throughout the entire reaction zone, confirm the behavior outlined above. However, there are several other cases, which don't have such simple descriptions. For example, there exist cases in which there are multiple match points in the shock polar plane. See Figs. 5 and 6. There is another case, which has only a match at a supersonic point on the HE polar, see Fig. 7. There are other cases in which there is no apparent match (at least without an intervening Prandlt-Meyer fan in the inert.) See Fig. 8.

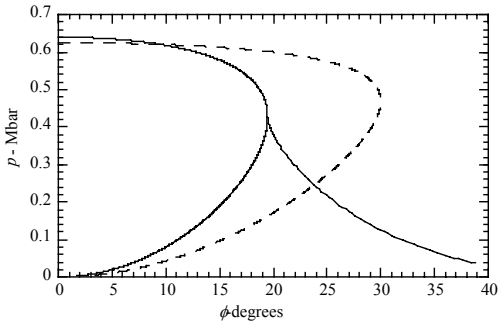

FIGURE 5. SHOCK POLAR WITH 2 POSSIBLE (ONE STRONG, ONE WEAK) MATCH POINTS. SOLID LINE IS HE POLAR (γ=3,ρo=2gm/cc,D_o=0.8cm/us), DASHED LINE IS INERT POLAR (γ=2,ρo=1.465gm/cc,D_o=0.8cm/us).

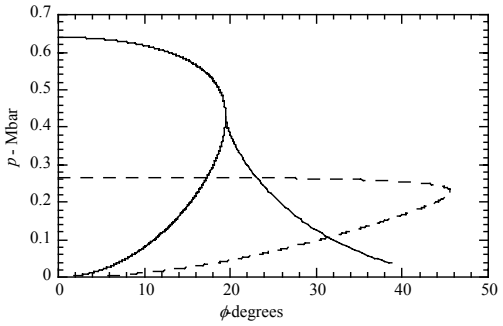

FIGURE 6. SHOCK POLAR WITH 3 POSSIBLE (ALL WEAK) MATCH POINTS. SOLID LINE IS HE POLAR (γ=3,ρo=2gm/cc,D_o=0.8cm/us), DASHED LINE IS INERT POLAR (γ=1.4,ρo=0.5gm/cc,D_o=0.8cm/us).

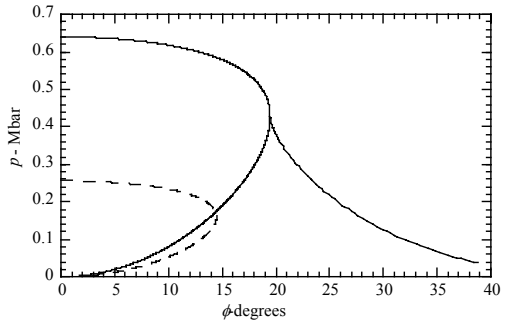

FIGURE 7. SHOCK POLAR WITH SUPERSONIC HE SHOCK MATCH POINT. SOLID LINE IS HE POLAR (γ=3,ρo=2gm/cc,D_o=0.8cm/us), DASHED LINE IS INERT POLAR (γ=4,ρo=1gm/cc,D_o=0.8cm/us).

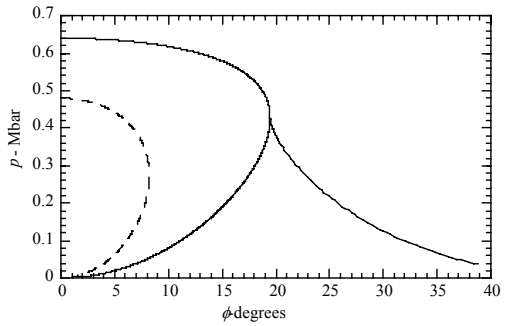

FIGURE 8. SHOCK POLAR WITH NO APPARENT MATCH POINT. SOLID LINE IS HE POLAR (γ=3,ρo=2gm/cc,D_o=0.8cm/us), DASHED LINE IS INERT POLAR (γ=7,ρo=3gm/cc,D_o=0.8cm/us).

The above shock polar diagrams represent some of the different types of interactions that can take place for steady propagating detonation waves. The focus of this work is to categorize all the types of interactions that are possible. In this paper, we present the results obtained using a high-resolution, multi-material, adaptive mesh refinement algorithm to compute the initial boundary value problems for the reactive Euler equations. This helps elucidate the large number of interactions that are possible. In cases where there exists more than one possible solution (for example Fig. 5), the type of interaction achieved depends on the thickness of the inert confining material. Also, the properties of any materials, adjacent to these thin inert confinement layers, are important.

Detailed analysis of the numerical simulations are presented, along with comparisons to the hydrodynamic theory. Where multiple solution types are possible, arguments based on hydrodynamic domain-of-dependence are presented that help to explain which solution type is realized.

COMPUTATIONAL RESULTS

Here, computational results will be presented that solve the two-dimensional Euler equations with reaction:

$$\rho_t + (\rho u)_x + (\rho v)_y = 0$$
$$(\rho u)_t + (\rho u^2 + p)_x + (\rho uv)_y = 0$$
$$(\rho v)_t + (\rho uv)_x + (\rho v^2 + p)_y = 0$$
$$E_t + (uE + up)_x + (vE + vp)_y = 0$$
$$(\rho\lambda)_t + (\rho u\lambda)_x + (\rho v\lambda)_y = \rho r$$

With an equation of state:

$$E = \frac{p}{\gamma - 1} - Q\rho\lambda + \frac{\rho}{2}\left(u^2 + v^2\right)$$

Here, a single reaction progress variable, λ, goes from zero (unreacted) to one (completely reacted) by the rate, r:

$$r = H(p_{ign})k(1-\lambda)^{1/2}$$

and

$$H(p_{ign}) = \begin{cases} 1, \text{ if } p > p_{ign} \\ 0, \text{ otherwise} \end{cases}$$

where p_{ign}=10kbar. We choose the following parameters for the HE: ρ_0=2 gm/cc, Q=4 mm^2/μs^2, k=2.5μs^{-1}, γ=3. This model gives a complete reaction zone (for the ZND-CJ detonation) of 4mm, with D_{CJ}=0.8cm/μs, and a ZND spike pressure of 0.64Mbar. All computations were performed using an Adaptive Mesh Refinement (AMR) strategy[1] to help deal with the multi-scale nature of detonation propagation[4]. We utilize the Ghost Fluid Method (GFM)[2] to treat the multi-material interfaces.

The computational problem will be to simulate a slab of explosive, 32mm in thickness and roughly 640mm in length, confined by a single inert. See Fig. 9. The left and right boundary conditions are rigid, while the upper and lower boundary conditions are zero gradient. The inert thickness will be taken to be 4mm, unless otherwise noted. Initially, a hot-region of HE will be used to trigger detonation. The numerical experiment is then run for several (usually near 20) charge widths, to ensure the solution has achieved a steady traveling state. In the next sections, computational results will be shown for the cases corresponding to Figures 2, 4 and 5.

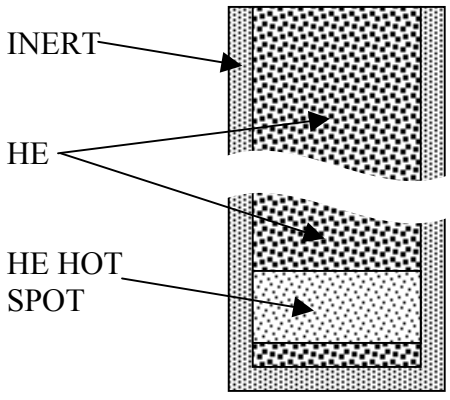

FIGURE 9. SCHEMATIC OF INITIAL CONDITIONS FOR NUMERICAL SIMULATIONS. NOTE THE TRUE ASPECT RATIO IS MUCH LARGER.

STRONG CONFINEMENT

Here, we choose the inert confining material to have the properties: ρ_0=9 gm/cc and γ=7. See Fig. 2 for the HE and inert shock polars. This gives a match in the shock polar plane with a pressure of 627kbar, and a streamline deflection of 7.9° and a detonation shock deflection angle of 8.2° (the shock deflection in the inert is 48.7°). In Figure 10, we see a pressure plot of the resulting numerical simulation. Clearly the shock polar analysis gives a good prediction for the HE-inert interaction.

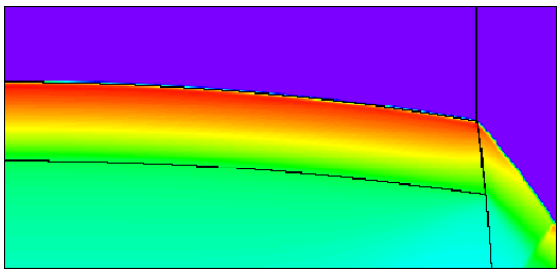

FIGURE 10. PRESSURE PLOT OF STRONG INERT CONFINEMENT. SOLID LINES REPRESENT MATERIAL INTERFACE AND SONIC LOCUS.

WEAK CONFINEMENT

Here, we choose the inert confining material to have the properties: ρ_0=2 gm/cc and γ=1.4. This gives a match in the shock polar plane with a pressure of 250kbar, and a streamline deflection of 23.6° and a detonation shock deflection angle of 35.3° (the shock deflection in the inert is 61°). In Figure 11, we see a density plot of the

resulting numerical simulation. Note the Prandlt-Meyer fan in the HE. Again, the shock polar analysis gives a good prediction for the HE-inert interaction.

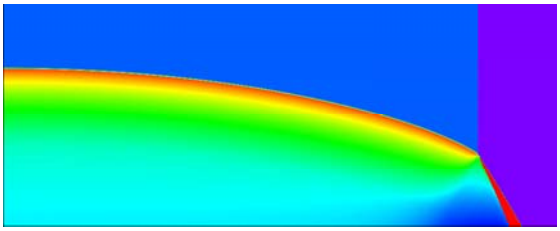

FIGURE 11. DENSITY PLOT OF WEAK INERT CONFINEMENT.

DUAL SHOCK POLAR MATCHES

Here, we choose the inert confining material to have the properties: ρ_0=1.465 gm/cc and γ=2. This gives the dual match in the shock polar plane, corresponding to Figure 5. The strong match yields a pressure of 620kbar, and a streamline deflection of 9.5° and a detonation shock deflection angle of 10.1° (the shock deflection in the inert is 4.9°). The weak match point yields a pressure of 245kbar, and a streamline deflection of 23.8° and a detonation shock deflection angle of 35.3° (the shock deflection in the inert is 51.2°). In performing a series of numerical studies, varying the thickness of the inert material, we find that if the material is relatively thick, when compared to the reaction zone length, the weak confinement match is seen. See Figure 12. Note that this is a steady traveling configuration, and the Mach stem that forms in the inert (next to the rigid confinement) does not propagate forward, So, it has no chance to catch up and influence the reaction zone. In other words, the subsonic portion of the reaction zone is completely surrounded by supersonic flow.

When the thickness of the inert is relatively thin, we see the strong confinement solution. See Figure 13. Here, there is a subsonic region behind both the detonation shock and the inert shock, and thus the reaction zone "feels" the affects of the outside rigid confinement.

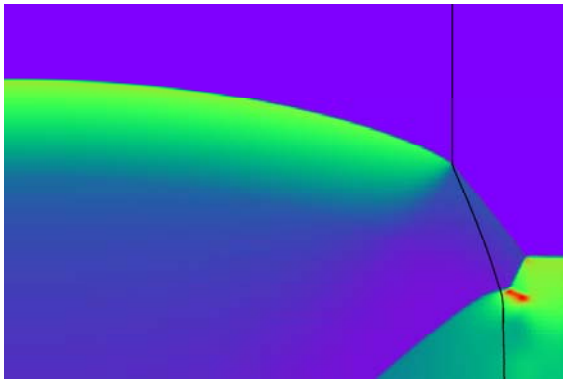

FIGURE 12. PRESSURE PLOT OF WEAK INERT CONFINEMENT (4mm thick inert).

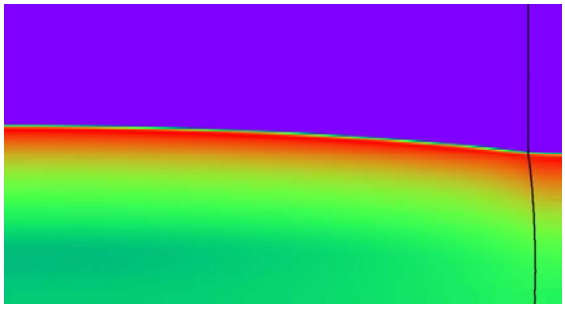

FIGURE 13. PRESSURE PLOT OF STRONG INERT CONFINEMENT (1mm thick inert).

Notice that the streamline deflection and pressure near the material interface are quite different between Figures 12 and 13. This difference affects the phase speed as well. Recall that the HE charge thickness (3.2 cm) is the same in these figures. Varying the thickness of this inert gives varying phase speeds. See Figure 14.

Also shown in Figure 14 is the variation of phase speed as a function of numerical resolution. Somewhere between 2mm and 3mm confiner thicknesses, one observes the transition from strong confinement to weak confinement. Once the weak confinement is reached, further increases in the thickness produce no further decreases in phase velocity (this is due to the fact that the reaction zone is completely surrounded by a supersonic region). As pointed out in Stewart and Bdzil[3], if the inert confiner is roughly greater than 1/2 a reaction zone length (in our case the reaction zone length is 4mm), it might as well be "infinitely thick", since no further information from beyond this distance has a chance at catching the detonation reaction zone. This is precisely where the transition is observed in this case.

On the other hand, the phase speed is sensitive to the thickness *when* the strong confinement case is achieved. Clearly, when the thickness is zero, and the second inert is truly rigid, one gets D_{CJ} as the phase speed for the steady traveling solution. When the thickness of the inert is finite, but thin enough to be a "subsonic" interaction, then this thickness plays a role.

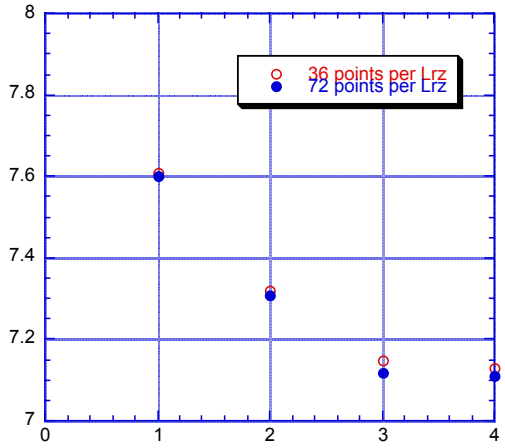

FIGURE 14. PHASE SPEED (mm/υs) VERSUS THICKNESS OF INERT CONFINER.

DISCUSSION

Here, it has been demonstrated that the inert confining material can have a profound affect on the local (and even global) behavior of high explosive-inert systems. It has also been demonstrated that the shock polar analysis can be used to accurately describe the HE-inert interaction at charge edges. As noted in Stewart and Bdzil[3], there can be many types of HE-inert interactions. In utilizing a theory, such as Detonation Shock Dynamics[3-6], it is critical to understand appropriate boundary conditions for propagating detonation shocks.

REFERENCES

1. Quirk, J.J., "A parallel adaptive grid algorithm for computational shock hydrodynamics," Applied Numerical Mathematics , Vol. 20, No. 4, 1996, pp. 427-453.

2. Fedkiw , R. P., Aslam, T.D., Merriman, B. and Osher, S. J., “A non-oscillatory Eulerian approach to interfaces in multimaterial flows (the ghost fluid method),” Journal of Computational Physics, Vol. 152, No. 2, 1999, pp. 457-492.

3. Stewart , D. S., Bdzil, J. B., “Examples of Detonation Shock Dynamics for Detonation Wave spread Applications,” Ninth Symposium (International) on Detonation, Vol. 152, No. 2, 1989, pp. 773-783.

4. Aslam T, Bdzil J, Hill L, "Analysis of Rate Stick Data for PBX9502," Eleventh International Detonation Symposium, August 1998, pp 21-29.

5. Aslam T, Bdzil J and Stewart D S, "Level Set Methods Applied to Modeling Detonation Shock Dynamics," Journal of Computational Physics, vol. 126, 1996, pp 390-409.

6. Bdzil, J., Aslam, T., Catanach, R., Hill, L. and Short, M., “DSD Front Models: Nonideal Explosive Detonation”, Twelfth International Detonation Symposium.